Journal of Fundamental and Applied Sciences

ISSN 1112-9867

Available online at http://www.jfas.info

Research Article

CORROSION BEHAVIOR OF API N80 STEEL MATERIAL IN ALBIEN WATER

F. Chelgham[1,*], N. Bouzid[2], M.Saidi[1], A. Boumaza[2], A. Taabouche[3], S .Boudjema[4]

[1]Laboratoire de Valorisation et Promotion des Ressources Sahariennes, Université Kasdi Merbah, 30000 Ouargla, Algeria

[2]Structures, Properties and Inter Atomic Interactions Laboratory (LASPI2A), Faculty of Science and technology, Unversity of Abbes Laghrour, Khenchela 40000, Algeria

[3]Thin Films and Interfaces Laboratory, University of Constantine 1, Constantine, Algeria

[4]Laboratoire de Catalyse et Synthèse en Chimie Organique, Faculté des sciences, University of Tlemcen 1300, Algeria

Received: 08 May 2018 / Accepted: 30 June 2018 / Published online: 01 September 2018

ABSTRACT

At Hassi-Messaoud, the recuperation of oil is assisted by injection of water extracted from Albian aquifer. To increase the injection capacity of the water, API N80 concentric has been installed along production wells, the difference between the temperature of the water wells and that of the water injected into the concentric generates a temperature gradient ΔT varying in depth and up to 16°C. The present study endeavors to examine, first the effect of tempering temperature on the corrosion behavior of API N80 pipe in Albian water at different temperature gradients and then to determine the nature of corrosion deposit. Polarizations results for samples tested at different ΔT shows a general decline in corrosion rate values with increase in tempering temperature. FTIR and XRD analysis revealed that corrosion scale is heterogeneous; the formation of various compounds depends strongly on temperature.

Keywords: API N80 pipe; temperature gradient; Albian water; FTIR; Corrosion Scale.

Author Correspondence, e-mail: fchelgham@gmail.com

doi: http://dx.doi.org/10.4314/jfas.v10i3.20

1. INTRODUCTION

Carbon steel is one of the most widely used in petroleum and gas industry. The materials K55, J55, L80, P110 and N80 are used as tubing material or geothermal well casings. The materials used for the transportation pipelines, the injection well casings and other equipment must be resistant to corrosion by injected gas/fluids. Carbon steels are vulnerable to corrosion in environment containing oil production. Corrosion in gas and oil pipelines is one of the most interesting operation problems to predict and control.

The dangers of corrosion, loss of production as a result crude oil or water may leak as a result of corrosion which may cause environmental and water pollution and the decrease in pipeline lifetime.

The API N80 pipe is of the material used as tubing in oil wells, due to their relatively low cost, good properties and easy fabrication. Several studies on API N80 pipe shows that it is used in well construction, and it has generally been used as the main construction material for downhole tubulars and transmission pipelines in the petroleum industry [1-4].

Corrosion behaviour of N80 carbon steel in formation water containing CO_2 was studied by S.D. Zhu and al. [4]. Effects of temperature on the corrosion behavior of N80 carbon steel were discussed. The results showed that increasing temperature not only enhanced the dissolution of steel substrate, but also promoted the precipitation of $FeCO_3$.

At Hassi-Messaoud (Haoud Berkaui region) , located about 100 km in south Algeria, the recuperation of oil is assisted by injection of water under pressure in the geological formation; this water is extracted from Albian aquifer by several producing wells drilled at depths of 1300 m. To increase the injection capacity of this water, API N80 concentric has been installed along production wells for the transport of treatment products.

The difference between the temperature of the water wells (60 °C at the bottom, 25 °C at the surface), and that of the water injected into the concentric (25 °C) generates a temperature gradient ΔT varying in depth and up to 16 °C.

The lifetime of concentric, initially predicted for five years, has been reduced to only two. The concentric back up from the wells was severely affected by corrosion. Corrosion of

carbon steel will depend on properties of the environment like pressure, pH, flow, temperature, etc. and the base alloy such as composition and microstructure [5].

Temperature can affect in many ways the corrosion of pipes. For a same quality of water, corrosion can be significantly different from a constant temperature to another. Pipes subjected to a variation in temperature (increasing or decreasing) corrode differently from those, which remain at constant temperatures.

Due to temperature changes, mechanical stresses may occur in pipes due to changes in temperature, mainly because the corrosion scales has different coefficient of thermal expansion than the metal [6]. The effect of temperature gradient on copper pipe corrosion during stagnant conditions was exanimate by J.C. Rushing and al. [7], these authors showed that gradient temperature of 20°C influences copper scale type.

The water temperature within a pipe can change throughout the year due to seasonal variations of the water source. Thus, a pipe may exhibit different corrosion behavior in the winter versus the summer. According to L. Fiksdal study, weight loss decreased for iron samples held at 13 versus 20 °C [8].

The aim of the present work was to study the combined action of the temperature gradient and tempering treatment on the corrosion of concentric pipes in Albian water. The determination of the nature of corrosion scale of pipe removed from wells after two years of operation was performed using FTIR spectroscopy and X-Ray diffraction. The first subtitle opens with an introduction that presents the specific problem under study and describes the research strategy.

2. EXPERIMENTAL

2.1. Water analysis

The water sample were taken at the head of producing water wells, the principal analyzed chemical factors were pH, calcium, magnesium, potassium, sodium, chlorides, bicarbonates, sulfates and nitrates.

2.2. Tempering treatment

API N80 pipeline steel, with a chemical composition (wt.%) C: 0.21%, Si: 0.1%, Mn: 0.75%, P: 0.007%, S: 0.007%, Mo: 0.05%, Cr: 0.12%, Cu: 0.16%, V: 0.01% and Fe: balance, were tempering for one hour at temperature ranging from 200 to 500 °C and subsequently cooling in oven, heating rate are 50°C/min. The samples were then polished up to 2000 grit wet abrasive paper, rinsed with distilled water and finally degreased in acetone.

2.3. Microhardness measurements

The hardness was determined by using Vickers microhardness tester with a load of 200 g applied for 15 seconds, HV values are an average of four measurements.

2.4. X-ray diffraction

The XRD analysis was carried using the PANalytical X'PERT Pro Philips diffractometer (λ = 1.54059 Å), the tension, intensity and the scanning rate are 34 KV, 22 mA, and 2°/mn, respectively. The XRD analysis of corrosion scales was carried out on powder scratched from the inner and outer surfaces of the pipe.

2.5. Electrochemical tests

The experimental measurements used for electrochemical studies are Potentiostat - galvanostat Type PGZ 301, connected to PC computer utilizing VoltaMaster-4 software.

The electrochemical cell is similar to a water-producing well, composed of a casing of production, where circulates the hot fluid (Albian water) ascending, and a concentric treatment where circulates the cold fluid descending.

The first cylinder (for containing water Albian) is composed of a glass tank of 30 x 20 x 20 cm dimension, provided with two holes for the introduction of the reference electrode in saturated KCl calomel and platinum auxiliary electrode section 1 cm^2 (figure 1). The second cylinder consists of a cylindrical tank, provided with an opening at the bottom where is placed on the working electrode, which was prepared from a representative sample of API 5CT N80, it was 14 cm^2 surface. The heating of the water of the two cylinders is ensured by two heating resistances, controlled by adjustable thermostats to ensure the control of the temperature.

Results processing is done using a software voltamaster4 allowing direct reading of the

corrosion current and the corrosion rate by the method of extrapolation of Tafel straight, the scan rate used was 30 mV / min. Electrolyte used is Albian untreated water recovered on site Haoud Berkaoui.

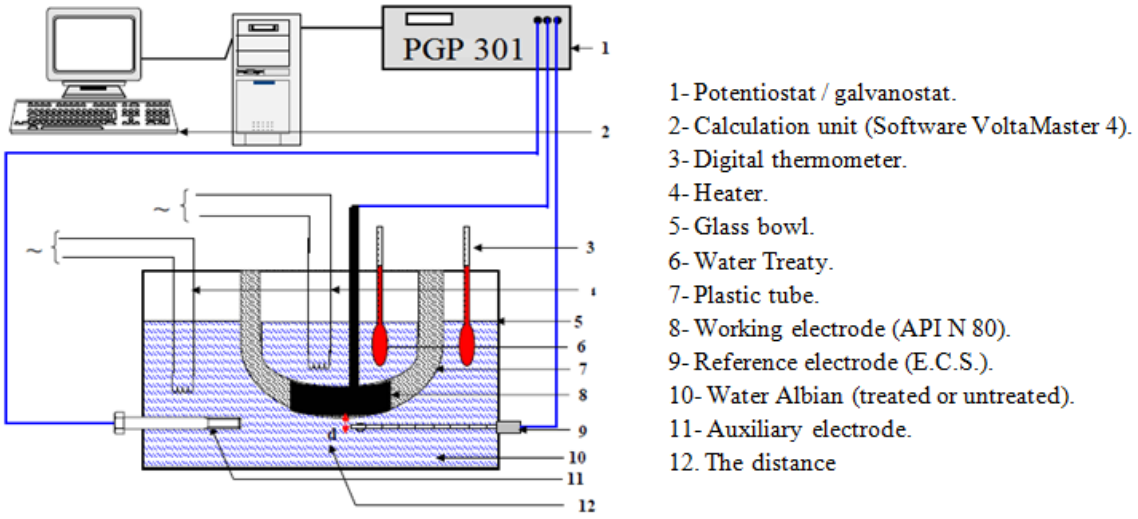

Fig.1. Schematic diagram of the apparatus

2.6. FTIR Analysis

FTIR spectra are obtained using a Perkin–Elmer spectrometer at the resolution of 8 cm^{-1}. Fourier transform infrared (FTIR) technique is used in the transmission mode in the 400 - 4000 cm^{-1} range. For each sample, 120 scans are used. After the sample cutting, ~ 5 mg of the oxides are scraped. The mineral is then compressed together with 23 ± 2mg of KBr in a cold 150 MPa isostatic press (CIP) in order to obtain a 200 - 250 µm thick pellet. All infrared spectra are reporting absorbance ($A= - \log (I/I_0)$) as a function of the incident wave numbers.

3. RESULTS AND DISCUSSION

3.1. Albian water chemical composition

The result of chemical analyze is represented in table 1, the water is chlorinated and rich in sulfates, its alkalinity is due to bicarbonates, the pH is slightly basic, pHs is the pH of water saturated with calcium carbonate.

Among the various indices likely to determine the corrosion of water and the formation of

scale, let us examine the Ryznar indice given by: RI= 2 pHs – pH and that of Langelier defined by: LI = pH – pHs. The values of these tow indexes (RI = 5.95 and LI = 0.92) shows the tendency of water to form scale.

Table 1. Chemical composition of Albian water

Elements %	**Ca^{+2}**	**Mg^{+2}**	**Na^{+}**	**K^{+}**	**Cl^{-}**	**SO_4^{-2}**	**HCO_3^{-}**	**NO_3^{-}**	**pH**	**pHs**
Composition (mg/l)	197	142	365	55	500	1107	189	1.3	7.79	6.87

3.2. Structural Properties

Figure 2 shows the XRD diagrams of the API N80 pipe untreated and tempered at different temperatures, the results show that the samples studied have a centered cubic ferrite structure (a=2.867Å, JCPDS file n°06-0696).The crystallite size (D) was estimate using the Scherrer formula: $D = 0.9\lambda/\beta\cos\theta$: Where λ,θ and β were the X-ray wavelength (λ = 1.54059 Å), Bragg diffraction angle and line width at half-maximum, respectively. The average grain sizes (D_{moy}) was calculated using the three most intense peaks.

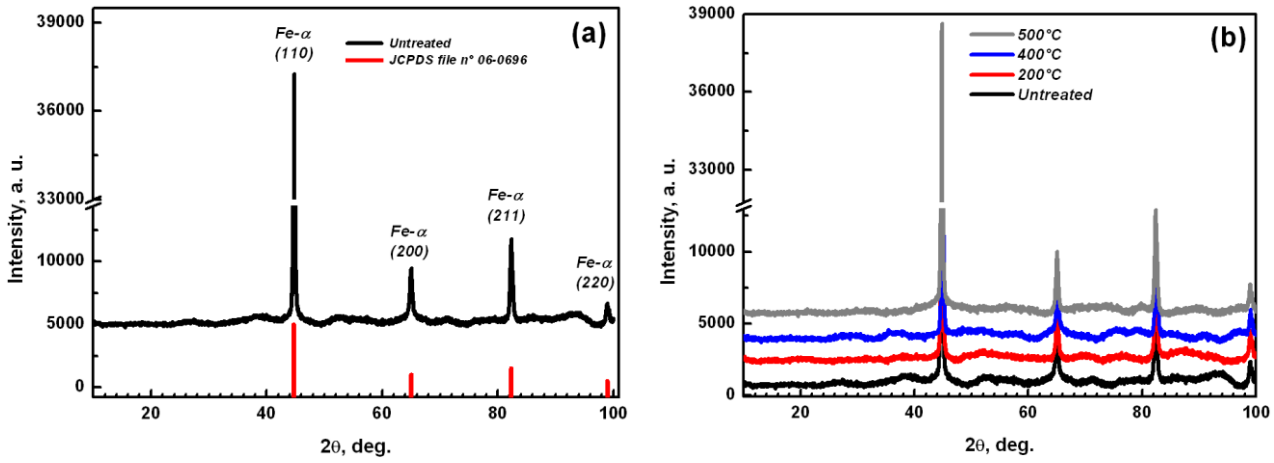

Fig.2. X-ray diffractions of API N80 untreated and tempered at different temperatures

In figure 3, we observe that the tempering treatment does not lead to significant variation in ferrite grain size (the corrosion rate increases with decreasing grain size due to defects

concentrated in grain boundaries) [9]. Figure 4 shows the variation of the microhardness as a function of tempering treatment: HV of untreated steel decreases as a function of the increasing tempering temperature, this lead to a softening of the material.

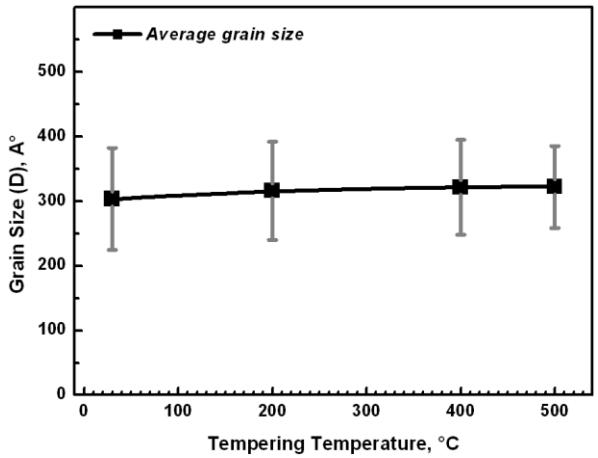

Fig.3. Relation between the average grain size and the tempering temperature

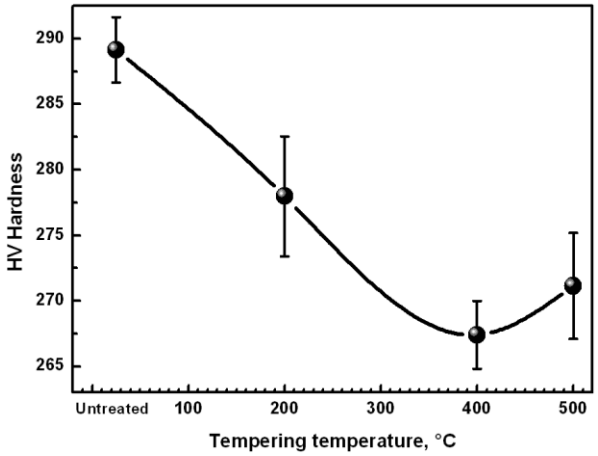

Fig.4. Relation between the microhardness and the tempering temperature

3.3. Electrochemical Experiments

The results of the electrochemical kinetic parameters (i corr, Ecorr, ba and bc) obtained from the Tafel graphs (Figures 5) for untreated steel and those having tempering treatments at different temperatures in presence of a temperature gradient are shown in Table 2.

Table 2. Polarization results for untreated and heat treated API N80 pipe

Temperature Gradient (°C)	Tempering temperature (°C)	E_{corr} (mv)	b_a (mv/dec)	- b_C (mv/dec)	I_{corr} (µAcm^{-2})	Corrosion rate V (µm/y)
	untreated	-676,3	74,6	104,6	5,6451	66,02
	200	-565.5	44.7	163.6	3.1637	37.00
ΔT= 0	400	-651.0	53.8	59.7	3.2252	37.72
	500	-567.4	58.8	263.7	4.7198	55.20
	untreated	-681,3	53,4	74,2	11,4212	133,5
	200	-677,6	50,0	76,6	11,0538	129,2
ΔT= 9	400	-680,8	59,0	78,3	9,1917	107,5
	500	-696,1	62,3	80,7	12,1969	142,6
	untreated	-696,9	76,1	114,7	16,1128	188,4
	200	-696,6	62,3	81,9	15,1511	177,2
ΔT= 16	400	-684,2	77,2	102,1	11,9362	139,6
	500	-689,1	66,7	89,0	15,9677	186,7

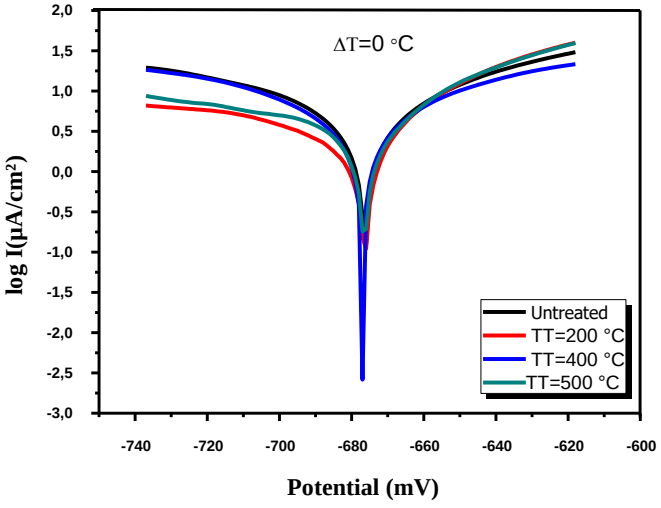

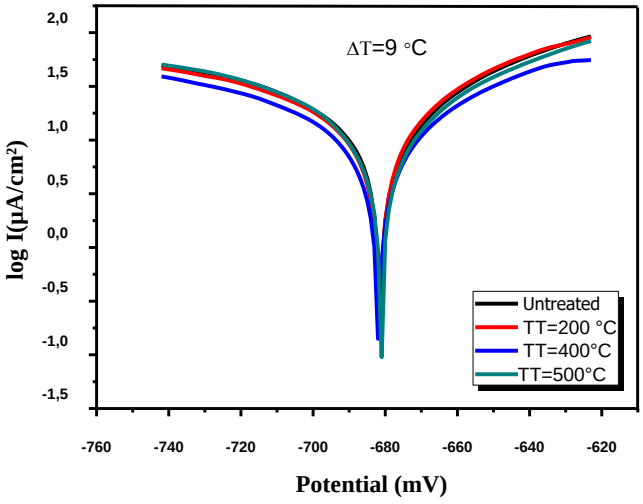

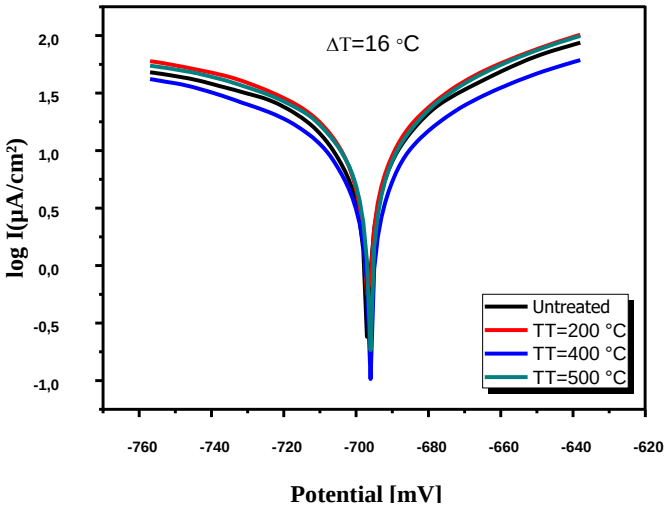

Fig.5. Polarization results for untreated and heat treated API N80 pipe in Albian water

Figure 5 represents the typical potentiodynamic polarization curve of API N80 pipe in Albian water at different temperature gradient, the corrosion current decreased with increasing tempering temperature.

Table 2 shows the Tafel parameters deduced from the polarization curves, the corrosion rates for untreated pipe were significantly higher than tempering temperature.

Polarizations results for samples tested at ΔT= 0, 9 and 16°C in Figure 6 shows a general decline in corrosion rate values with increase in tempering temperature (except for 500°C).

The temperature gradient (to which API N80 pipe is subjected under the actual conditions of exploitation of the Albian water producing wells) causes a not insignificant increase of corrosion rate; the steel tends to be low resistant to corrosion with increase in gradient temperature.

For Albian water, the effect of the Cl^- ion seems more deleterious than SO_4^{-2} due to its relatively small size and strong electronegativity thus accelerating the dissolution rate of the steel. It must be noted that the presence of Cl^- and SO_4^{2-} ions accelerated the redox electrochemical mechanisms responsible for corrosion [10]

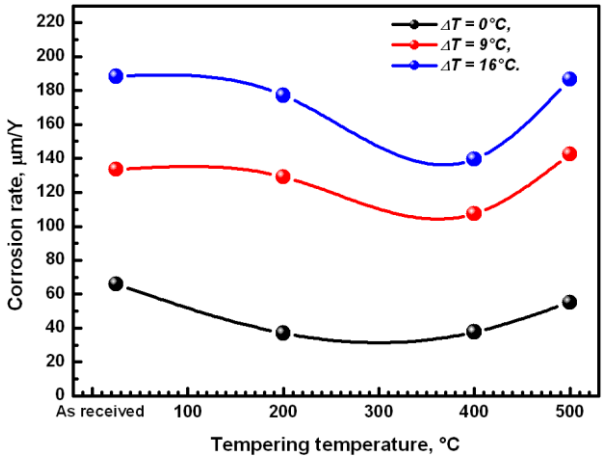

Fig.6. Corrosion rate versus tempering temperature at different temperature gradient

3.4. Corrosion scales analysis

3.4.1. Fourier Transform Infrared (FTIR) analysis

The various samples analyzed by FTIR spectroscopy allowed us to characterize a corrosion scale depending on whether this phenomenon took place inside or/and outside the API N80 pipe. The importance of FTIR spectroscopy is due to the fact that it is sensitive to all products whether they are amorphous or crystalline. It should be recalled that we compared these oxides, carbonates, sulphates, and complex mixtures with laboratory products that served to have the reference FTIR spectra, which has the advantage of having results under the same recording conditions as those of our corrosion products.

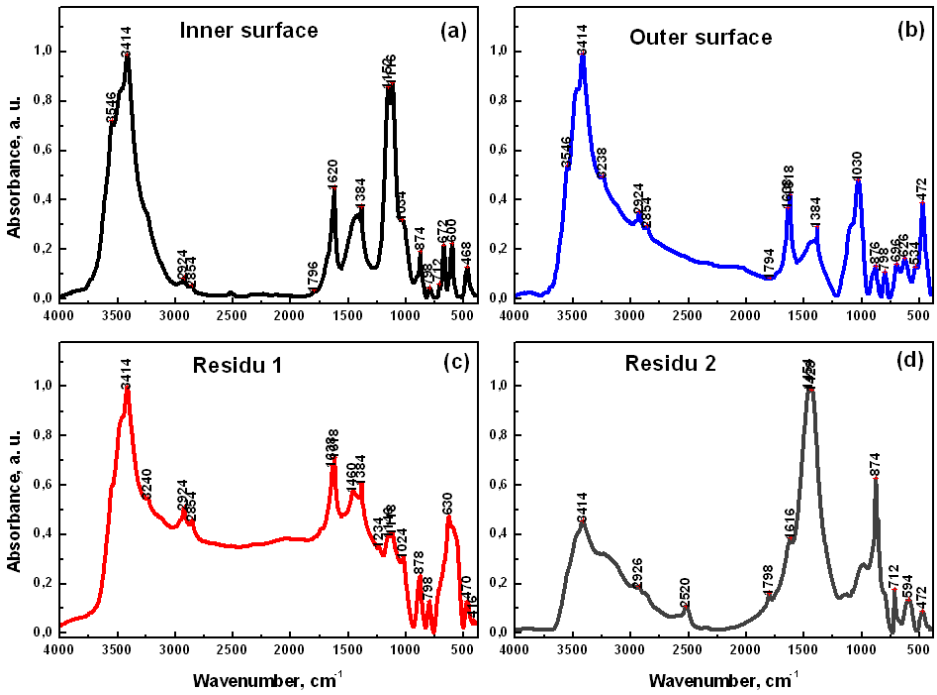

Fig.7. FTIR absorption spectra of corrosion scales of (a) Inner surface, (b) outer surface, (c) residu1, (d) residu2

Figures 7a and 7b shows the FTIR absorbance spectra of corrosion scales collected on the inner and outer part of the pipe. Figure 7c and 7d are those of corrosion scales collected on areas severely affected, we call those scales residu1 and residu2. In Figures 8a, 8b, 8c, and 8d we have superimposed on the different spectra FTIR of samples analyzed, those of the following compounds: $CaSO_4$, $CaMg(CO_3)_2$, SiO_2 and $FeCO_3$ for comparison. The FTIR absorbance spectra of $CaSO_4$, and $CaMg(CO_3)_2$ are similar to those of corrosion scales of API N80 inner surface in range of 500–3800 cm^{-1} indicating the presence of similar functional groups. The corrosion scales of inner surface has peaks at 468, 600, 672, 712, 798, 874, 1034, 1116, 1152, 1384, 1620, 1796, 2854, 2924, 3414 and 3546 cm^{-1}. The outer surface part has peaks at, 472, 534, 626, 696, 798, 876, 1030, 1384, 1618, 1638, 1794, 2854, 2924, 3238, 3414, and 3546 cm^{-1}. Peaks at 880 and 1384 cm^{-1} indicate the presence of nitrate groups. Figure 8c shows that residu1 contain similar compounds to those formed in the outer part of API N80 pipe, to which is added the broad absorption band between 550 and 750 cm^{-1}, that we can assign to C-S or C-Cl . For résidu2, comparing the FTIR spectra of Figure 8d provides a very

good satisfaction, residu2 appears to contain $FeCO_3$ and $CaMg(CO_3)_2$. We observe also the presence of quartz which is revealed by the absorbance peaks at 470 cm^{-1}, and 800 cm^{-1}.

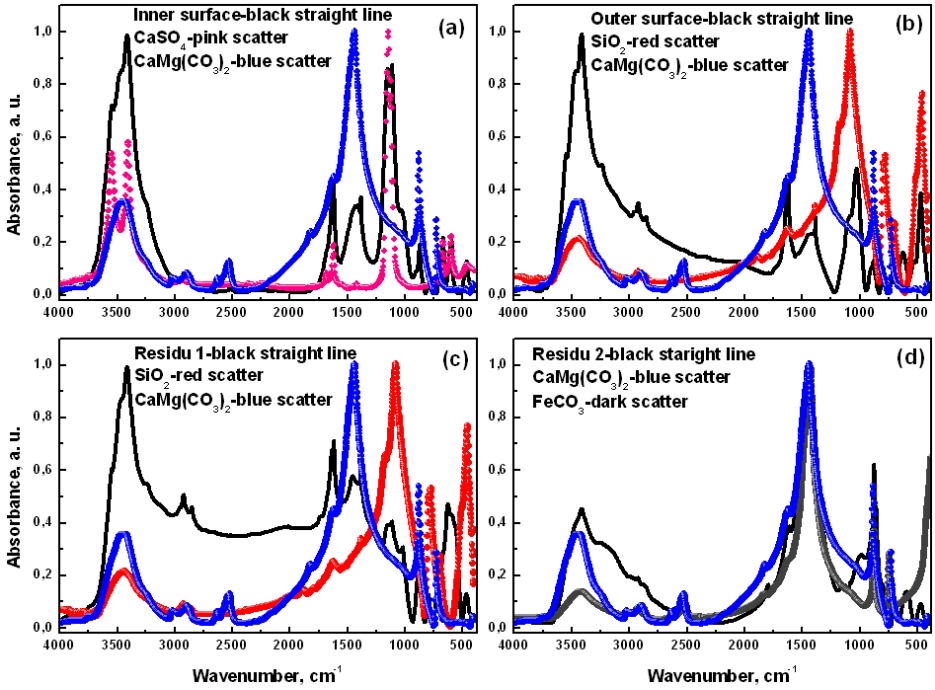

Fig.8. FTIR absorption spectra of corrosion scales of: **(a)** Inner surface with FTIR spectra of $CaSO_4$ and $CaMg(CO_3)_2$, **(b)** outer surface with FTIR spectra of SiO_2 and $CaMg(CO_3)_2$, **(c)** residu1 with FTIR spectra of SiO_2 and $CaMg(CO_3)_2$, **(d)** residu2 with FTIR spectra of $FeCO_3$ and $CaMg(CO_3)_2$

The band assignments of the fundamental modes for the scales found on API N80 pipe are given in table3

Table 3. Band assignments of the fundamental vibrational modes in sulfate minerals, carbonate minerals, nitrates, SiO_2 minerals mineral and other chemical groups (in cm^{-1})

Chemical groups/mineral	Absorption bands	ref
CO_3^{2-}	728-880-1438-1618-1822-2524-2628	[11-13]
SO_4^{2-}	602-674-1122-1145-1620	[11-13]
Si-O, Si-O-Si (SiO_2)	458-694-778-796-1082-1168-1624	[18]
NO_3^-	880-1384	[14]
CH_2 – (ν_s, ν_{as})	2854-2924	[15]
Adsorbed water	1638-3020-3548	[16,17]

To reveal the presence of iron-oxides in corrosion scales, we exploited the FTIR spectra in the zone between 400 and 900 cm^{-1}(figure 9), which represents the finger-print region of these minerals [19, 20]. The hematite characterized by an absorbance around 470 cm^{-1}; except that this line may overlap with the quartz line. The magnetite is given by the FTIR absorbance towards 800 - 890 cm^{-1}, the goethite is given by the FTIR absorbance towards 800 - 890 cm^{-1}, it's found in residu1, inner and outer part of API N80 pipe.

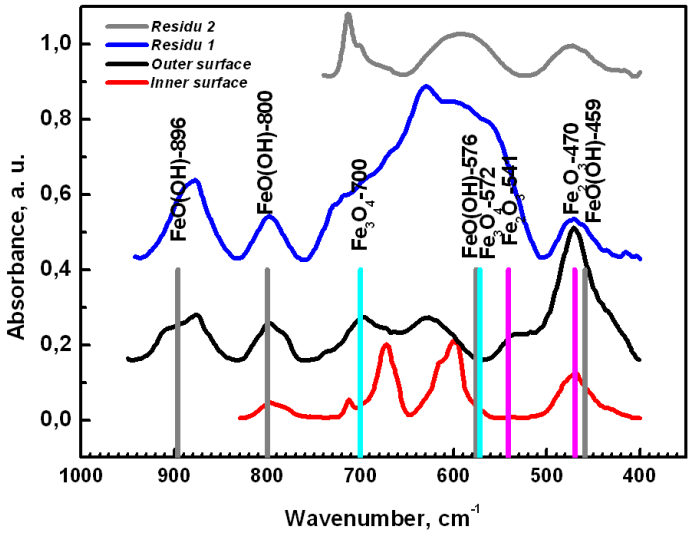

Fig.9. FTIR absorption spectra of corrosion scales in the finger –print region of hematite(Fe_2O_3), magnetite (Fe_3O_4) and goethite(FeO(OH))

3.4.2. X-ray diffraction analysis

The XRD patterns of the corrosion scales of inner surface, outer surface, residu1 and residu2, is shown in Figure 10. Fe_3O_4, Fe_2O_3,FeO(OH), $FeCO_3$, $CaCO_3$, and $CaSO_4$ crystalline compounds were found (JCPDS files n°03-862, 03-0800, 17-0536, 02-0837, 03-0569, and 37-1496 respectively). The quartz SiO_2 was found only on the outer surface, (JCPDS file n°02-0471), the water that flows outside of the pipe is not filtered, so it contains quartz which comes from the soil. Due to the presence of Ca^{2+}, SO_4^{2-} and HCO_3^-, formation of $CaSO_4$ and $CaMg(CO_3)_2$ or $CaCO_3$ are expected. Major peaks for Fe_3O_4 were observed in figures 10 (a), 10 (c) and 10 (d) corresponding to the inner surface, residu1 and residu2. The results obtained by DRX corroborate those of FTIR analysis: the corrosion scale is heterogeneous and composed from the same compounds found by Z.Tang and al. [21] in the study conducted on unlined cast iron after contact with varying water quality (blends of ground, surface and saline waters) for one year; the quality of water alone cannot explain the variation in corrosion behavior [22].

For API N80 pipes and Albian water quality, the formation of various compounds depends strongly on temperature which is variable along depth of wells: The increase of temperature causes a decrease in the viscosity, leading the increase of transport of reactants and product from and to the metal surface, so an increase in corrosion rate [23-27].

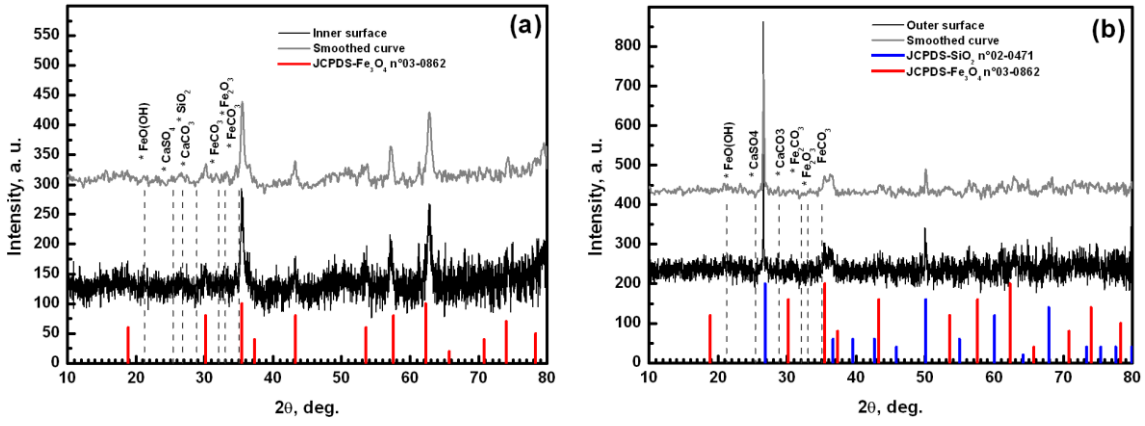

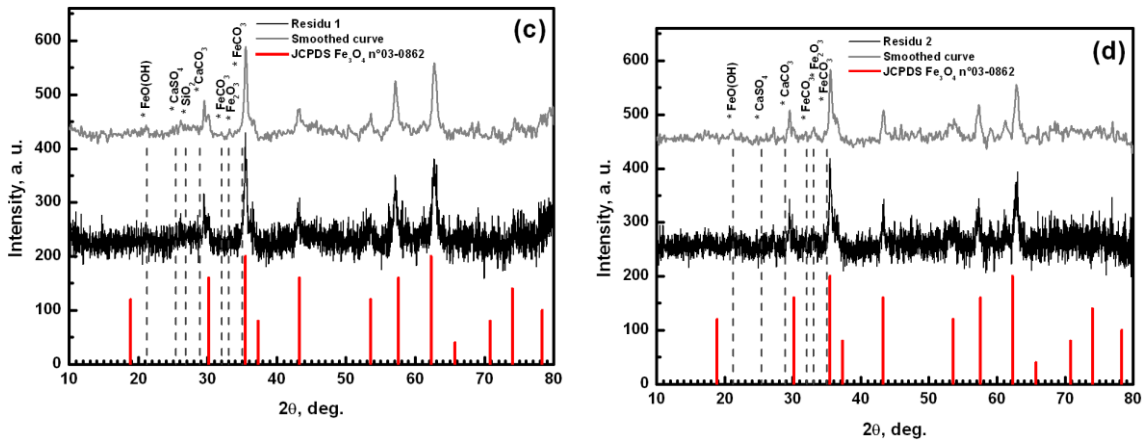

Fig.10. XRD patterns of corrosion scales of: (a) Inner surface, (b) outer surface, (c) residu1, (d) residu2.

Moreover the ferrous iron oxidation rate and thermodynamic properties (activity coefficient, solubility, etc) of specific ions of Albian water are also affected by change in temperature. These changes can affect significantly the nature of corrosion scales, the deposit is heterogeneous, and as a result the physical properties of corrosion scale changes when temperature varies. Different scale component have different coefficient of thermal expansion (α_i given in table 4) and different densities (ρ_i) compared to the metal or other layers of scale. The rate of expansion or contraction between the various compounds of corrosion scales was estimated using the following relation:

$$\tau_{i/j}(\%) = \frac{\left(\frac{\Delta l}{l_0}\right)_i - \left(\frac{\Delta l}{l_0}\right)_j}{\left(\frac{\Delta l}{l_0}\right)_j} = \frac{\alpha_i \Delta\theta_i - \alpha_j \Delta\theta_j}{\alpha_j \Delta\theta_j}$$

Iron metal (α=12.5$\times 10^{-6}$ °C) will expand and contract nearly 46 % more than Fe_2O_3 scale (α=8.35$\times 10^{-6}$ °C) and 40% more than Fe_3O_4 scale (α=8.92$\times 10^{-6}$ °C) in response to the same temperature change ($\Delta\theta_i = \Delta\theta_j$). The greater the disparity between expansion coefficients, the less adherent the oxide becomes when temperature varies, mechanical stresses are thus created in the scale.

Table 4. Thermal expansion coefficients α_i

Mineral/oxyde	**Feα**	**Fe_3O_4**	**Fe_2O_3**	**$FeCO_3$**	**FeO(OH)**	**$CaSO_4$**	**$CaMg(CO_3)_2$**
α (10^{-6} °C^{-1}) [20-100°C]	12,5	8.92	8.53	64,4	2.3-4.05	7.22	28.05

Furthermore, The PBR ratios given by the relation: $PBR = \frac{\rho_M M_{M_xO_y}}{x m_M \rho_{M_xO_y}}$ is 2.14 for Fe/Fe_2O_3, 2.10 for Fe/Fe_3O_4 and 1.018 for Fe_2O_3/Fe_3O_4. PBR is greater than one, as a consequence compressive stresses are present in scales oxide, depending on the surface geometry (more greater for concave or convex surfaces). The stress can lead to scale spalling and crack formation, the surfaces of pipes (inner or outer) are not protected, they are thus exposed to the solution, as a consequence the corrosion rate increase. Figure11 shows the condition of the pipe after 2 years of operation, the internal and external parts of the latter are severely affected by corrosion.

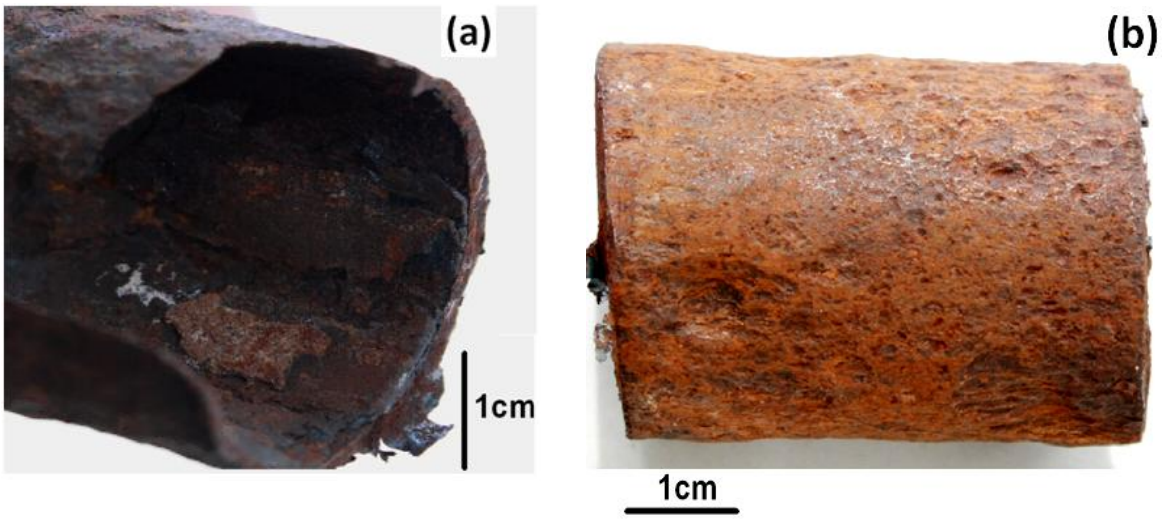

Fig.11. Macrographic views of the pipe states for: (a) inner surface, (b) outer surface

4. CONCLUSION

In order to understand the effect of temperature on the corrosion behavior of API N80 steel, series of experiments were carried out; the main results of this study can be summarized as follows:

1) It was found that softening of API N80 pipe occurred, hardness decreases as a function of the increasing tempering temperature.

2) The results of potentiodynamic polarization indicate a general decline in corrosion rate values and the corrosion current decreased with increase in tempering temperature

3) The temperature gradient played a significant role in the corrosion of N80 steel in albian water environment, the steel tends to be low resistant to corrosion with increase in gradient temperature, the corrosion rate reached maximum value at 16 °C.

4) Based on FTIR and XRD results, Fe_2O_3, Fe_3O_4, FeO(OH), $FeCO_3$, $CaMg(CO_3)_2$ or $CaCO_3$, $CaSO_4$ and SiO_2 were identified as primary corrosion products of API N80 pipes. The formation of one or another of the various compounds depends strongly on temperature which affects their physicals properties such as density and coefficient of thermale expansion; these changes lead to scale spalling and crack formation, thus accelerate corrosion phenomena.

5. ACKNOWLEDGEMENTS

The authors gratefully the Laboratoire des couches Minces et Interfaces (LCMI) of Frères Mentouri University -Constantine algeria for financial support.

6. REFERENCES

[1] Matjazˇ F., Ennifer J., Application of corrosion inhibitors for steels in acidic media for the oil and gas industry, Corros. Sci., 2014, 86,17-41, doi : 10.1016/j.corsci.2014.04.044

[2] Yadav M., Behera D., SharmaU., Nontoxic corrosion inhibitors for N80 steel in hydrochloric acid, Arab. J. Chem , 2012, 9 (2) S1487-S1495, doi :10.1016/j.arabjc.2012.03.011

[3] Vishwanatham S., Haldar N., Furfuryl alcohol as corrosion inhibitor for N80 steel in hydrochloric acid , Corr. Sci., 2008, 50 (11) 2999-3004, doi:10.1016/j.corsci.2008.08.005

[4] Zhu S.D., Fu A.Q., J. Miao, Yin Z.F., Zhou G.S., Wei J.F., Corrosion of N80 carbon steel in oil field formation water containing CO2 in the absence and presence of acetic acid, Corr. Sci. , 2011, 53 (10) 3156-3165, doi:10.1016/j.corsci.2011.05.059

[5] Lopez D.A., Perez T., Simison S.N., The influence of microstructure and chemical composition of carbon and low alloy steels in CO2 corrosion. A state-of-the-art appraisal, Mater. Desi. ,2003,24 (8) 561-575, doi:10.1016/S0261-3069(03)00158-4

[6] McNeill L.S., Edwards M.,The importance of Temperature in assessing Iron Pipe Corrosion in Water Distribution Systems, Environ. Monit. Assess.,2002,77(3), 229-242.

[7] Rushing J.C., Edwards M., The Role of Temperature gradients in Residential Copper Corrosion, Corros. Sci., 2004,46(8), 1883-1893, doi:10.1016/j.corsci.2003.11.001

[8] Fiksdal L. ,Water Quality and Internal Corrosion of Iron Pipes, in Proceedings of Internal Corrosion in Water Distribution Systems, Goteborg, Sweden, 1995,111-115.

[9] Di schino A., Kenny J. m., Effects of grain size on the corrosion behavior of refined AISI 304 austenitic stainless steels, J. Mater. Sci. Lett., 2002, 21(20)1631-1634

[10] Loto R. T., Aiguwurhuo O., Evana U., Corrosion Resistance Study of Heat Treated 420 Martensitic Stainless Steel and 316 Austenitic Stainless Steel in Dilute Acid Concentrations, Rev. Téc. Ing. Univ. Zulia., 2016, 39(7)35-40, doi:10.21311/001.39.7.04

[11] Andriashin V. A., Kostyuchenko A. A., Komarov A. I. , Vorobs'ev V. V. , Long-term inside corrosion attack of an oil main operation, Prot. Met., 2006, 42(1) 46-50.

[12] Sridhar N., Dunn D.S., Anderko A.M., Lencka M.M., Schutt H.U., Effects of Water and Gas Compositions on the Internal Corrosion of Gas Pipelines, Modeling and Experimental Studies, Corr. J , 2001, 57(3), 221-235, doi: 10.5006/1.3290347

[13] Tavanpour N., Noshadi M., Tavanpour N., Scale Formation and Corrosion of Drinking Water Pipes: A Case Study of Drinking Water Distribution System of Shiraz City, Moder. Appl. Sci., 2016, 10(3), doi:10.5539/mas.v10n3p166

[14] Destainville A., Champion E., Bernache-Assollante D., Laborde E.,Synthesis, characterization and thermal behaviour of apatite tricalcium phosphate, Mater. Chem. Phys., 2003, 80(1), 269 -277, doi:10.1016/S0254-0584(02)00466-2

[15] Ramesha S., Rajeswari S., Maruthamuthu S., Corrosion inhibition of copper by new triazole phosphonate derivatives, Appl.Surf.Sci., 2004,229(1-4),214-225, doi:10.1016/j.apsusc.2004.01.063

[16] Raynaud S., Champion E., Bernache-Assollant D. , Thomas P. , Calcium phosphate

apatite with variable Ca/P atomic ratio I. Synthesis, characterisation and thermal stability of powders, Biomater.,23(4), 1065-1072, doi:10.1016/S0142-9612(01)00218-6

[17] Meejoo S., Maneeprakorn W., Winotai P., Phase and thermal stability of nanocrystalline hydroxyapatite prepared via microwave heating, Thermochim. Acta , (2006), 447(1), 115-120, doi:10.1016/j.tca.2006.04.013

[18] Ullah R., Deb B. K., Mollah M.Y.A., Synthesis and Characterization of Silica Coated Iron-Oxide Composites of Different Ratios, Inter. J. of Composite Mater.,2014, 4(2): 135-145, doi: 10.5923/j.cmaterials.20140402.13

[19] Kim Y.S., Kim J.G., Corrosion Behavior of Pipeline Carbon Steel under Different Iron Oxide Deposits in the District Heating System, Metals ,2017, 7(5), 182, doi:10.3390/met7050182

[20] Liang J., Deng A. , Xie R., Gomez M., Hu J., Zhang J.,Choon Nam Ong a, Avner Adin, Impact of seawater reverse osmosis (SWRO) product remineralization on the corrosion rate of water distribution pipeline materials, Desalination ,2013, 311, 54-61 ,doi:10.1016/j.desal.2012.11.010

[21] Tang Z., Hong S., Xiao W., Taylor J., Characteristics of Iron Corrosion Scales Estabilished under Blending of Ground, surface and Saline Waters and their Impacts on Iron Release in the Pipe Distribution System,Corr. Sci., 2006,48(2),322-342 , doi:10.1016/j.corsci.2005.02.005

[22] McNeill L.S., Edwards M., Iron Pipe Corrosion in Drinking Water Distribution Systems, J. Am. Water Works Assoc., 2001, 93(7), 88-100

[23] Davalos J., Garcia M., Marco J.F. , Grancedo J.R., Corrosion of Weathering Steel and Iron under Wet-dry Cycling Conditions, Influence of the Rise of Temperature During the Dry Period, Hyperfine Interact. , 1991, 69(1-4), 871-874

[24] Mabuchi K., Horii Y., Takahashi H., Nagayama M., Effect of Temperature and Dissolved Oxygen on the Corrosion Behavior of Carbon steel in High-temperature water, Corr. J, 1991, 47(7), 500-508, doi:10.5006/1.3585285

[25] Bouzid N., Settou N., Lanez T., Djelloul A., Bebba A. A. ChelghamF. Rôle des transferts thermiques sur la corrosion des concentriques utilisés dans les puits producteurs d'eau

albienne, Revue des sciences de l'eau / Journal of Water Science, 2009, 22, (3), 397-406

[26] Zaiz T., Lanez T. Application of some ferrocene derivatives in the field of corrosion inhibition. Journal of Chemical and Pharmaceutical Research, 2012, 4(5):2678-2680.

[27] Toumiat K., Guibadj A., Taouti M.B., LaneZ T. Electrochemical study and computational details of cop**p**er corrosion inhibition by 1h-benzotriazole in 3 % wt. NaCl medium, Mor. J. Chem. 2015, 3(2) 809-823

How to cite this article:
Chelgham F, Bouzid N, Saidi M, Boumaza A, Taabouche A and Boudjema S. Corrosion behavior of api n80 steel material in albien water. J. Fundam. Appl. Sci.. 2018. 10(3). 300-319.